Microchim Acta (2016) 183:2353–2359
DOI 10.1007/s00604-016-1876-6

ORIGINAL PAPER

Colorimetric determination of lysozyme based on the aggregation of gold nanoparticles controlled by a cationic polymer and an aptamer

Xin Yao[1] · **Xiangdong Ma**[1] · **Chun Ding**[1] · **Li Jia**[1]

Received: 1 March 2016 / Accepted: 18 May 2016 / Published online: 26 May 2016

Abstract We report on a colorimetric lysozyme (LZ) assay that is based on the aggregation of gold nanoparticles (AuNPs) induced by poly(diallyldimethylammonium chloride) (PDDA) and an LZ-specific 25-base aptamer. The method is based on the finding that AuNPs undergo aggregation on addition of PDDA. If, however, aptamer is present, it will undergo electrostatic interaction with PDDA to form a duplex structure. Hence, the aggregation of AuNPs is suppressed. Upon the addition of LZ, the aptamer will bind to LZ to form a complex. Subsequent addition of PDDA causes the aggregation of 20-nm AuNPs which is accompanied by a color change from red to blue. Based on this color change, LZ can be determined qualitatively with bare eyes, and quantitatively by photometry by measuring the absorbance ratio at 590 and 531 nm. The calibration plot is linear in the 4.4 to 200 nM LZ concentration range, and the detection limit is 4.4 nM (at an S/N ratio of 3). The method was successfully employed to the determination of LZ in egg white. Results were compared to those of an established method and gave recoveries between 95.8 and 115 %, with RSDs of <3.9 %.

Keywords Nanomaterial · Photometric assay · Visual test · Ratiometric measurement · Aggregation assay · Dynamic light scattering

Electronic supplementary material The online version of this article (doi:10.1007/s00604-016-1876-6) contains supplementary material, which is available to authorized users.

✉ Li Jia
jiali@scnu.edu.cn

[1] Ministry of Education Key Laboratory of Laser Life Science & Institute of Laser Life Science, College of Biophotonics, South China Normal University, Guangzhou 510631, China

Introduction

Lysozyme (LZ) is an alkaline globulin that consists of 129 amino acid residues, which is present in mammalian body fluids including saliva, plasma, tears, milk, urine, and in egg white at a high level. The protein is considered as a powerful bactericide because it can destroy bacterial cell walls by catalyzing the hydrolysis of 1, 4-β-linkages between the muramic acid and *N*-acetylglucosamine of the mucopolysaccharides [1]. Because LZ possesses immune-boosting, anti-viral, anti-inflammatory and other pharmacological activities, it has been applied as a potential marker in the diagnosis of disease [2, 3]. It has been discovered that the concentration of LZ in serum and urine is closely related with leukemia [4], renal diseases [5], and meningitis [6]. In addition, LZ has also been used as a biological preservative in food industry [7]. For example, fresh vegetables, cheese, and wine have been preserved by coating the surface of the food with LZ or adding LZ to the food [8]. Thus, the detection of LZ has received more and more attention in practical applications.

So far, various methods such as fluorescence spectrometry [9, 10], fluorescence resonance energy transfer [11], surface plasmon resonance [12], resonance Rayleigh scattering [13], electrochemistry [14], high efficiency liquid chromatography [15], chemiluminescence in combination with molecularly imprinting technique [16] and so on have been developed for the quantitative analysis of LZ. Nevertheless, these methods need special equipments for performance, which limit their on-site detecting applications. Thus, it is desired to develop a fast, sensitive, selective, and instrument-free method for LZ detection.

It is well known that gold nanoparticles (AuNPs) have strong plasmon absorption at around 520 nm with a high

extinction coefficient, possess large surface areas, excellent biocompatibility, as well as distance-dependent optical properties. Based on these properties, AuNPs can be used as an important type of colorimetric indicator, which depends on a color change from red to blue corresponding to their dispersion or aggregation [17–19]. Various AuNP-based colorimetric systems have been established to detect ions, oligonucleotides, proteins and other small molecules [20–26] due to the advantages of low cost, simplicity and practicality. Especially, color changes can be read out by the bare eye and colorimetric biosensing does not require expensive or sophisticated instrumentation and may be applied to on-site analysis.

Several AuNP-based colorimetric sensors have been developed for detection of LZ [27–29]. Chen et al. reported that AuNPs covalently bonded with human serum albumin (HSA) were used for sensing LZ based on the electrostatic interaction between positively charged LZ and negatively charged HSA-capped AuNPs [27]. In the method, the time-consuming process for preparation of HSA-capped AuNPs (more than 12 h) was required. Wang et al. [28] reported that aptamer-immobilized PDMS-AuNPs composite film was coupled with silver enhancement colorimetric technique for LZ detection, which revealed high sensitivity and selectivity for LZ. However, aptamer needed to be immobilized on PDMS and the preparation of aptamer-immobilized PDMS-AuNPs composite film took 12 h. As we all know, aptamers, which are similar to antibodies, have high affinity and specificity for their targets. Based on the property of aptamer, Su et al. reported another colorimetric method for selective detection of LZ, in which, LZ-induced charge reduction of the negatively charged LZ DNA aptamer can potentially stabilize the cysteamine-capped AuNPs and prevent electrostatic assembly of the AuNPs on the aptamers and the color change of the AuNP solution [29].

We developed a colorimetric method for LZ detection based on the aggregation of unmodified AuNPs mediated by a cationic polymer, poly(diallyldimethylammonium chloride) (PDDA), and an LZ-specific aptamer. Positively charged PDDA can trigger the aggregation of negatively charged AuNPs via the electrostatic attraction. In the presence of LZ aptamer, PDDA interacts with aptamer through electrostatic attraction to form a duplex structure, which prevents the aggregation of AuNPs. In the presence of LZ, LZ aptamer specifically binds to LZ to form an LZ-aptamer complex. Thus the following addition of PDDA can induce the aggregation of AuNPs and cause a distinct color change from red to purple and blue. Based on the above observations, we aimed at developing a simple, sensitive, and selective colorimetric method for LZ detection. The method does not involve modification of AuNPs and requirement of expensive or sophisticated instrumentation.

Experimental

Materials and reagents

Tetrachloroauric (III) acid hydrate ($HAuCl_4 \cdot H_2O$) was acquired from Sinopharm Chemical Reagents Company (Shanghai, China, www.sinoreagent.com). Trisodium citrate ($Na_3C_6H_5O_7 \cdot 2H_2O$) was purchased from Guangdong Guanghua Sci-Tech Company (Shantou, China, www.jinhuada.com). PDDA was obtained from Sigma-Aldrich Company (Saint Louis, MO, USA, http://sigmaaldrich.guidechem.com). Nitric acid (HNO_3) was purchased from Luoyang Chemical Reagents Factory (Luoyang, China). Phosphoric acid (H_3PO_4) was purchased from Tianjin Damao Chemical Reagent Factory (Tianjin, China, www.chemreagent.net). Disodium hydrogen phosphate dodecahydrate ($Na_2HPO_4 \cdot 12H_2O$) and sodium dihydrogen phosphate dihydrate ($NaH_2PO_4 \cdot 2H_2O$) were obtained from Guangzhou Chemical Reagents Factory (Guangzhou, China, www.chemicalreagent.com). Cytochrome c (Cyc, Mw 12.4 kDa, pI 10.2) and ribonuclease A (Rnase A, Mw 13.7 kDa, pI 9.3) were purchased from Sigma-Aldrich Company (Saint Louis, MO, USA, www.sigmaaldrich.com). LZ (Mw 14.4 kDa, pI 11.1) was purchased from GBCBIO Technologies Company (Guangzhou, china, www.gbcbio.cn). Bovine serum albumin (BSA, Mw 67 kDa, pI 4.8) was purchased from Shanghai Bio Science & Technology Company (Shanghai, China, www.bio-rad.com). Chicken eggs were obtained from a local supermarket. The sequence of LZ aptamer, 5′-CCTGGGGGAGTATTGCGGAGGAAGG-3′, was synthesized by Sangon Biotechnology Co. Ltd. (Shanghai, China, www.sangon.com). The water (18.2 Ω · cm) used throughout the experiments was purified by an Elga water purification system (ELGA, London, UK, www.elgalabwater.com).

UV-vis absorption spectra were recorded by Microspectrophotometer (K5600, Beijing Kaiao Technology Development Company, Beijing, China, www.bjko.com.cn). Transmission electron microscopy (TEM) images were carried out on a JEM-2100HR transmission electron microscope (JEOL, Tokyo, Japan, www.jeoluk.com). A Zetasizer Nano ZS (Malvern, Worcestershire, UK) was employed to measure the average size of AuNPs and Stokes-Einstein formula was used as a mathematical model for dynamic light scattering analysis.

Preparation and characterization of AuNPs

AuNPs were synthesized by citrate reduction of $HAuCl_4$ [30]. Firstly, all glassware were cleaned with freshly prepared aquaregia (HCl-HNO_3, 3:1 [*v/v*]) and rinsed thoroughly with water. Then $HAuCl_4$ aqueous solution (1 mM, 100 mL) was heated to boiling and trisodium citrate solution (38.8 mM,

10 mL) was added quickly under stirring. The color of the solution changed quickly from pale yellow to wine-red within 1 min, and heating was continued for 20 min. Afterwards, the solution was cooled to room temperature and stored at 4 °C. The concentration of AuNPs was determined to be 2.6 nM by UV-vis spectroscopy according to the previously reported method [31].

Colorimetric detection of LZ

First, 50 μL AuNP solution (2.6 nM) was added to a 1.5 mL Eppendorf tube containing 10 μL LZ aptamer solution (0.6 μM) in 10 mM phosphate solution (pH 7.5). The mixture was shaken for 30 min. Then 290 μL LZ solutions (in 10 mM phosphate solution, pH 7.5) at different concentrations were respectively added to the mixture and incubated for 20 min at room temperature. Afterwards, 6 μL PDDA solution (111.1 nM) was added and the mixed solution was shaken for 60 s. Subsequently the UV-vis absorption spectra of the solution were recorded. The concentration of phosphate in the mixed solution was 8.4 mM.

In each experiment for optimization of LZ determination conditions, the samples were prepared in triplicate and each was measured three times. Standard deviations were used for error bars in Figs. 5, 6 and S2–S6.

Pretreatment of egg white sample

The sample was pretreated according to the previously reported method [32]. Briefly, egg white was diluted with 10 mM phosphate buffer (pH 7.5) in a 1: 20 ratio. The diluted egg white solution was mechanically agitated in an ice bath for 6 h. The resulting solution was further centrifuged at 10,000 r min^{-1} (9167 × g) and 4 °C for 30 min. Then, the supernatant was diluted 1000 times and used as the LZ resource. In order to demonstrate the reliability of the method, the recoveries of LZ were examined by standard addition method. All measurements were repeated three times and the relative standard deviation (RSD) was calculated to determine the reproducibility.

Results and discussion

Mechanism of the colorimetric sensing LZ

A schematic representation of the colorimetric assay towards LZ is illustrated in Fig. 1. Due to the coordination between Au and nitrogen atoms of single-strand DNA (ssDNA), the aptamer attaches to the surface of AuNPs. In the absence of LZ, PDDA can efficiently remove ssDNA (aptamer) from the AuNPs and hybridize with aptamer having a random coil

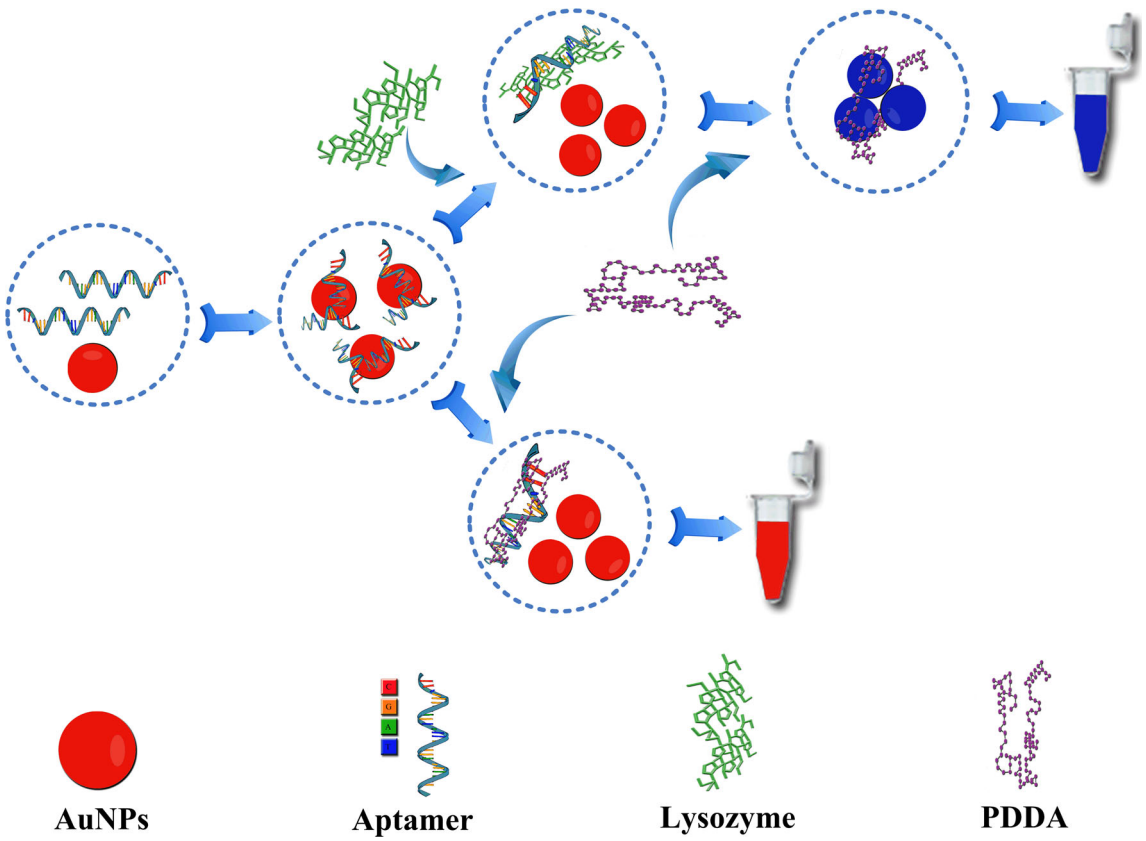

Fig. 1 Schematic illustration of the principle for LZ detection based on the aggregation of AuNPs mediated by PDDA and LZ aptamer

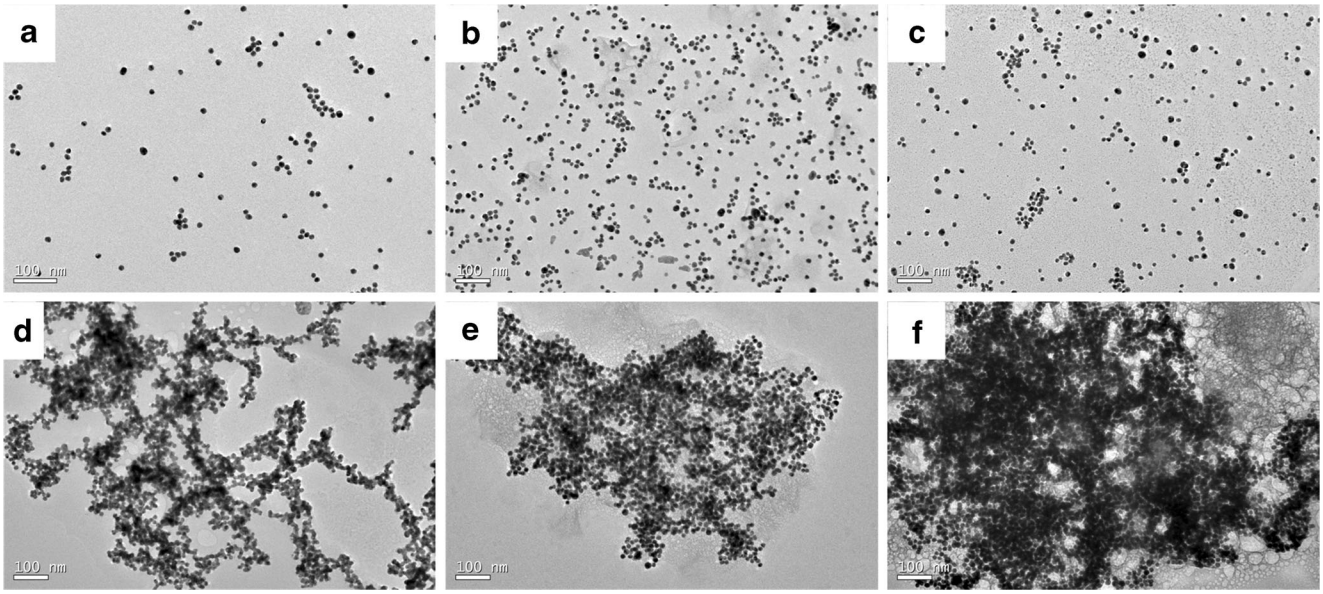

Fig. 2 The TEM images of AuNPs in different composition of solutions. **a** 0.365 nM AuNPs. **b** AuNPs + 0.6 μM LZ aptamer. **c** AuNPs + 0.6 μM LZ aptamer + 111.1 nM PDDA. **d** AuNPs + 111.1 nM PDDA. **e** AuNPs + 0.6 μM LZ aptamer + 111.1 nM PDDA + 100 nM LZ. **f** AuNPs + 0.6 μM LZ aptamer + 111.1 nM PDDA + 200 nM LZ

structure to form a duplex structure through electrostatic attraction [33]. In this case, PDDA is not sufficient to induce the aggregation of AuNPs and the solution color is red. However, once LZ is introduced, the aptamer specifically binds to LZ through a folded secondary structure, whose rigid structure prevents the exposure of aptamer bases to AuNPs. Thus, the subsequent addition of PDDA can aggregate the released AuNPs and cause the distinct color change from red to blue. While nontarget proteins do not elicit any change in color. These color change signatures can be used in the sensing of LZ for both qualitative recognition with the bare eye and quantitative analysis with a spectrometer.

Characterization of the colorimetric sensing system

UV-vis spectroscopy, dynamic light scattering and TEM analysis were used to characterize the colorimetric sensing system. As shown in Fig. 2a, the TEM images of AuNPs demonstrated that AuNPs were spherical, about 18 nm in diameter. The AuNP solution (0.365 nM, 0.356 mL) were used for the dynamic light scattering analysis. As shown in Fig. S1, the average size of AuNPs was 20.2 nm, which was in good agreement with the result of TEM analysis, indicating that AuNPs dispersed well. Addition of aptamer in the AuNP solution did not induce the aggregation of AuNPs. The AuNPs adsorbing negatively charged aptamer via the coordination between Au and nitrogen atoms in aptamer dispersed well because of electrosteric stabilization, as shown in Fig. 2b. When PDDA was added to the AuNP solution containing aptamer, aptamer prevented PDDA from inducing the aggregation of AuNPs since aptamer would form a duplex structure with PDDA via electrostatic interactions (Fig. 2c). In the absence of aptamer, addition of PDDA to the AuNP solution would trigger the tremendous aggregation of AuNPs through electrostatic interaction (Fig. 2d). Addition of PDDA to the AuNP solution containing the aptamer and LZ causes the aggregation of AuNPs since aptamer favors special binding to LZ, as shown in Fig. 2e and f. The UV-vis spectra of AuNPs (Fig. 3) showed an apparent peak shift towards higher wavelength at 590 nm due to the aggregation of AuNPs triggered by PDDA in the presence of LZ, which caused the visible color change from red to purple and blue. With the increasing of the

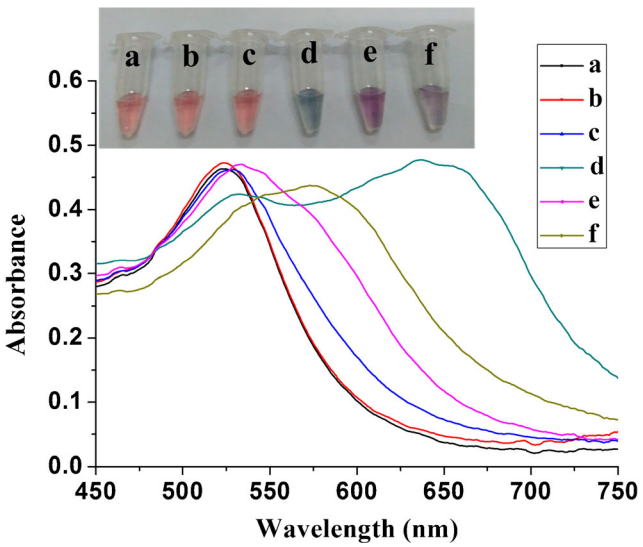

Fig. 3 The UV-vis spectra of AuNPs in different composition of solutions. **a** 0.365 nM AuNPs. **b** AuNPs + 0.6 μM LZ aptamer. **c** AuNPs + 0.6 μM LZ aptamer + 111.1 nM PDDA. **d** AuNPs + 111.1 nM PDDA. **e** AuNPs + 0.6 μM LZ aptamer + 111.1 nM PDDA + 100 nM LZ. **f** AuNPs + 0.6 μM LZ aptamer + 111.1 nM PDDA + 200 nM LZ

concentration of LZ, the aggregation degree of AuNPs increased since more aptamer interacted with LZ.

Optimization of method

The following parameters were optimized: (a) concentrations of PDDA; (b) concentrations of aptamer; (c) incubation times. Respective data and Figures are given in the Electronic Supporting Material. The following experimental conditions were found to give best results: (a) A PDDA concentration of 111.1 nM; (b) An aptamer concentration of 0.6 μM; (c) An incubation time of 60 s.

Sensitivity of LZ detection

Under the optimized conditions, the sensitivity of this method for LZ was researched. With the increase of LZ concentration, the absorbance of AuNP solution at 590 nm gradually increased, accompanied by a slight decrease of the absorbance intensity at 531 nm, as shown in Fig. 4. Owing to the change in the intensity ratio of the two absorbance peaks, the visible color of the AuNP solution changed continuously from red to purple and blue along with the increase of LZ concentrations (Fig. 4), which revealed that the color change was relevant with the concentration of LZ. Therefore, it is feasible to realize the qualitative detection of LZ by the bare eye using the present assay. When plotting the absorption ratio (A_{590}/A_{531}) against the LZ concentration (C), a good linear relationship was found (Fig. 5), which was expressed as an equation, $A_{590}/A_{531} = 0.0029C + 0.46$ ($R = 0.9964$). The lowest detectable concentration of LZ was 4.4 nM and the linear range was 4.4–200 nM using an UV-vis spectrometer.

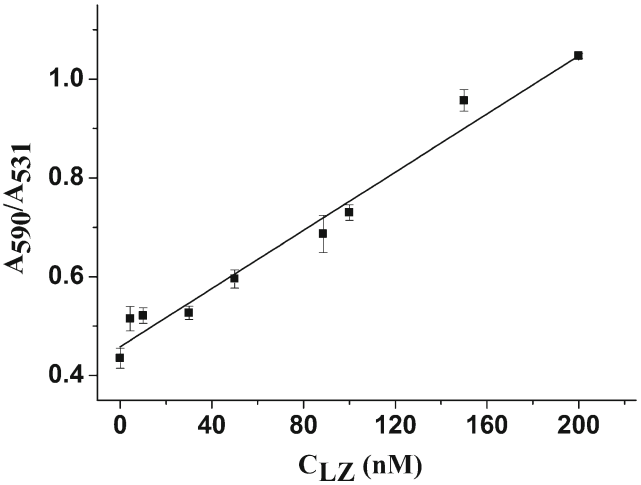

Fig. 5 The calibration curve for LZ determination ($n = 3$). Experimental conditions: 50 μL AuNPs (2.6 nM). 10 μL LZ aptamer (0.6 μM); 6 μL PDDA (111.1 nM); LZ concentration, 0, 4.4, 10, 30, 50, 88.6, 100, 150, and 200 nM, respectively

Selectivity of the biosensing system for LZ

Firstly, BSA, Cyc, and Rnase A were selected as the comparative proteins to verify the specificity of the biosensing system towards LZ. As demonstrated in Fig. 6, a significant change both in visual color and in absorption ratio at 590 and 531 nm was observed upon the addition of LZ. However, no or just a little change occurred in the presence of other competitive proteins with the same

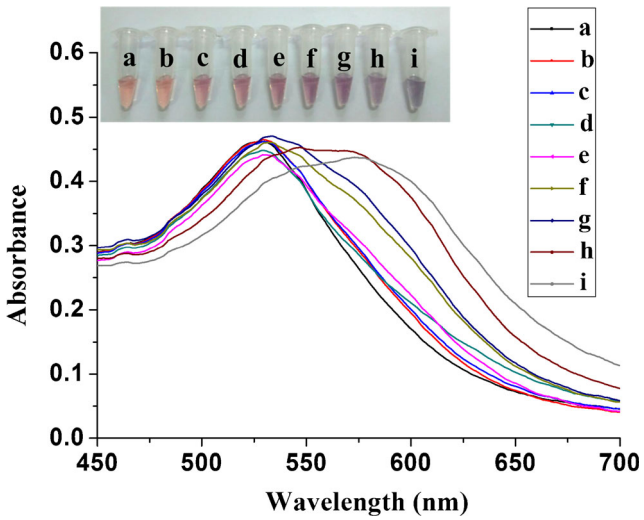

Fig. 4 UV-vis absorption spectra of AuNP solutions after addition of different concentrations of LZ. The inset shows the corresponding photographs. Experimental conditions: 50 μL AuNPs (2.6 nM). 10 μL LZ aptamer (0.6 μM); 6 μL PDDA (111.1 nM); LZ concentration from a to i, 0, 4.4, 10, 30, 50, 88.6, 100, 150, and 200 nM, respectively

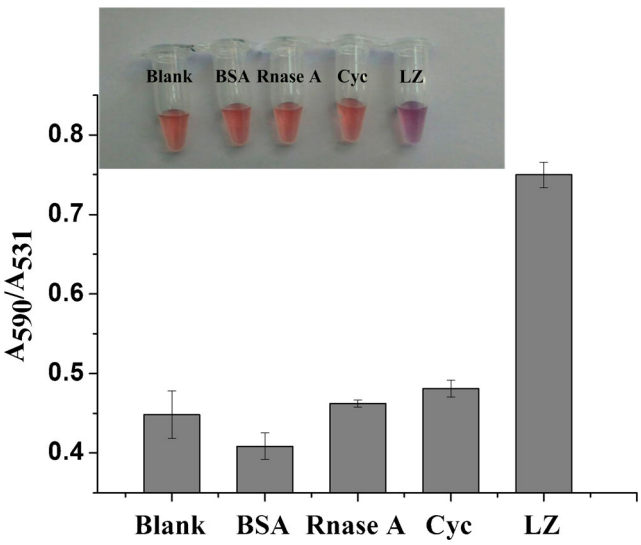

Fig. 6 Absorption ratios (A_{590}/A_{531}) of AuNP solutions after addition of comparative proteins and corresponding photographs ($n = 3$). The concentration of each protein was 100 nM. The inset shows the corresponding photographs

Table 1 Analytical results of LZ in diluted egg white and spiked samples

Sample	Added (nM)	Concentration found (nM)			Mean (nM)	Recovery (%)	RSD (%) ($n = 3$)
		1	2	3			
1	0	12.2	13.0	13.1	12.8	–	3.9
2	13	28.2	26.6	27.8	27.7	115	3.0
3	40	52.9	50.6	49.8	51.1	95.8	3.1

concentration of LZ. The results validated the selectivity of the biosensing system towards LZ detection.

Secondly, L-cysteine and glutathione (GSH) were used as model thiols to perform interference study since AuNPs are easy to interact with sulfydryl group to form Au-S bond. As shown in Fig. S5, in comparison with the blank, the obvious increase in the absorption ratio (A_{590}/A_{531}) of AuNP solution was observed upon addition of L-cysteine (100 nM) or GSH (100 nM). The result indicated that 100 nM thiols interfered with the LZ determination. We wondered whether lower concentrations of thiols influenced the detection of LZ. Thus, different concentrations of L-cysteine or GSH were respectively added to the LZ solutions (100 nM) to carry out the interference study. As shown in Fig. S6, when the concentration of L-cysteine or GSH was 22.3 nM, the absorption ratio (A_{590}/A_{531}) of AuNP solution did not happen to change, which demonstrated that L-cysteine or GSH with the concentration less than 22.3 nM did not interfere with the LZ determination. While, when the concentration of L-cysteine or GSH was more than 44.5 nM, the absorption ratios (A_{590}/A_{531}) of AuNP solutions obviously increased, which indicated that the LZ determination was interfered.

Application in egg white sample

Egg white was used to evaluate the feasibility of the colorimetric biosensing method in real samples. LZ-spiked egg white sample solutions were prepared by adding different concentrations of LZ to the diluted egg white samples. The recovery and reproducibility (RSD) of LZ from the spiked egg white samples were calculated and presented in Table 1. As shown in Table 1, the LZ concentration in egg white was 3.86 mg mL^{-1}, which is in good agreement with the reported normal values of LZ in egg white [34]. The recoveries varied from 95.8 to 115 % with RSD less than 3.9 %, which indicated that the present method was feasible to realize the rapid, selective and sensitive detection of LZ in egg white.

Conclusion

We have successfully developed a rapid, selective and sensitive colorimetric biosensing system for LZ determination based on the aggregation of AuNPs that is mediated by the interaction among PDDA, aptamer and LZ. In the system, PDDA not only can induce the aggregation of AuNPs, but can also hybridize with aptamer through electrostatic attraction. In comparison with most of previously reported methods aiming at the LZ detection (Table 2), the method demonstrated superiority in detection sensitivity. Although the detection limit (LOD) of the colorimetric method [28] is far better than that in our work, the preparation of aptamer-immobilized PDMS-AuNPs composite film (12 h) is time-consuming. The present method did not take time to immobilize aptamer on the AuNPs and the detection can be finished in less than 1 h. Furthermore, the method exhibited response towards LZ in real sample (egg white). However, the method is not suitable for the samples containing more than 44.5 nM thiols.

Table 2 Figures of merits of various methods for LZ detection

Techniques	LOD (nM)	Sample	Ref.
Fluorescence spectrometry	20	No	[10]
Fluorescence resonance energy transfer	54	Human urine	[11]
Surface plasmon resonance	70	No	[12]
Resonance Rayleigh scattering	0.045	Egg white	[13]
Liquid chromatography	56	Egg white	[15]
Colorimetry (HSA- AuNPs)	50	Egg white	[27]
Colorimetry (aptamer-immobilized PDMS-AuNPs composite film)	0.0069	No	[28]
Colorimetry (cysteamine-capped AuNPs)	35	No	[29]
Colorimetry (AuNPs)	4.4	Egg white	This work

Acknowledgments We are grateful to the financial support of the National Natural Science Foundation of China (21175048) and Natural Science Foundation of Guangdong Province, China (2015A030311013).

Compliance with ethical standards The authors declare that they have no competing interests.

References

1. Li Z, Cao M, Zhang W, Liu L, Wang J, Ge W, Yuan Y, Yue Y, Li R, Yu WW (2014) Affinity adsorption of lysozyme with Reactive Red 120 modified magnetic chitosan microspheres. Food Chem 145: 749–755
2. Ishii H, Iwata A, Oka H, Sakamoto N, Ishimatsu Y, Kadota J (2010) Elevated serum levels of lysozyme in desquamative interstitial pneumonia. Intern Med 49:847–851
3. Schroeder S, Stuerenburg HJ, Escherich F, Pfeiffer G, Schroeder F (2000) Lysozyme in ventriculitis: a marker for diagnosis and disease progression. J Neurol Neurosurg Psychiatry 69:696–709
4. Levinson SS, Elin RJ, Yam L (2002) Light chain proteinuria and lysozymuria in a patient with acute monocytic leukemia. Clin Chem 48:1131–1132
5. Harrison JF, Lunt GS, Scott P, Blainey JD (1968) Urinary lysozyme, ribonuclease, and low-molecular-weight protein in renal disease. Lancet 1:371–375
6. Klockars M, Reitamo S, Weber T, Kerttula Y (1978) Cerebrospinal fluid lysozyme in bacterial and viral meningitis. Acta Med Scand 203:71–74
7. Cunningham FE, Proctor VA, Goetsch SJ (1991) Egg-white lysozyme as a food preservative: an overview. World Poult Sci J 47:14–63
8. Mine Y, Ma F, Lauriau S (2004) Antimicrobial peptides released by enzymatic hydrolysis of hen egg white lysozyme. Food Chem 52: 1088–1094
9. Jiang CQ, Li L (2004) Lysozyme enhanced europium-metacycline complex fluorescence: a new spectrofluorimetric method for the determination of lysozyme. Anal Chim Acta 511:11–16
10. Liu S, Na W, Pang S, Shi P (2014) A label-free fluorescence detection strategy for lysozyme assay using $CuInS_2$ quantum dots. Analyst 139:3048–3054
11. Wang J, Liu B (2009) Fluorescence resonance energy transfer between an anionic conjugated polymer and a dye-labeled lysozyme aptamer for specific lysozyme detection. Chem Commun 17:2284–2286
12. Vasilescu A, Gaspar S, Mihai I, Tached A, Litescu SC (2013) Development of a label-free aptasensor for monitoring the self-association of lysozyme. Analyst 138:3530–3537
13. Cai ZX, Chen GX, Huang X, Ma MH (2011) Determination of lysozyme at the nanogram level in chicken egg white using resonance Rayleigh-scattering method with Cd-doped ZnSe quantum dots as probe. Sens Actuators B 157:368–373
14. Liu DY, Zhao Y, He XW, Yin XB (2011) Electrochemical aptasensor using the tripropylamine oxidation to probe intramolecular displacement between target and complementary nucleotide for protein array. Biosens Bioelectron 26:2905–2910
15. Pellegrino L, Tirelli A (2000) A sensitive HPLC method to detect hen's egg white lysozyme in milk and dairy products. Int Dairy J 10:435–442
16. Jing T, Xia H, Guan Q, Lu WH, Dai Q, Niu JW, Lim JM, Hao QL, Lee Y, Zhou YK, Mei SR (2011) Rapid and selective determination of urinary lysozyme based on magnetic molecularly imprinted polymers extraction followed by chemiluminescence detection. Anal Chim Acta 692:73–79
17. Zhang YF, Li BX, Chen XL (2010) Simple and sensitive detection of dopamine in the presence of high concentration of ascorbic acid using gold nanoparticles as colorimetric probes. Microchim Acta 168:107–113
18. He Y, Zhang XH, Yu HL (2015) Gold nanoparticles-based colorimetric and visual creatinine assay. Microchim Acta 182:2037–2043
19. Xu Q, Du S, Jin GD, Li HB, Hu XY (2011) Determination of acetamiprid by a colorimetric method based on the aggregation of gold nanoparticles. Microchim Acta 173:323–329
20. Jiang ZL, Fan YY, Chen ML, Liang AH, Liao XJ, Wen GQ, Shen XC, He XC, Pan HC, Jiang HS (2009) Resonance scattering spectral detection of trace Hg^{2+} using aptamer-modified nanogold as probe and nanocatalyst. Anal Chem 81:5439–5445
21. Zhan SS, Wu YG, He L, Wang FZ, Zhan XJ, Zhou P, Qiu SY (2012) A silver-specific DNA-based bio-assay for Ag (I) detection via the aggregation of unmodified gold nanoparticles in aqueous solution coupled with resonance Rayleigh scattering. Anal Methods 4:3997–4002
22. Lee JO, Kim EJ, Lim B, Kim TW, Kim YP (2015) Rapid detection of protein phosphatase activity using Zn (II)-coordinated gold nanosensors based on his-tagged phosphopeptides. Anal Chem 87:1257–1265
23. Luo YL, Liu X, Guo JJ, Gao HT, Li Y, Xu JY, Shen F, Sun CY (2016) Visual screening and colorimetric determination of clenbuterol and ractopamine using unmodified gold nanoparticles as probe. J Nanosci Nanotechnol 16:548–554
24. Huang H, Li L, Zhou GH, Liu ZH, Ma Q, Feng YQ, Zeng GP, Tinnefeld P, He ZK (2011) Visual detection of melamine in milk samples based on label-free and labeled gold nanoparticles. Talanta 85:1013–1019
25. Song Y, Wei W, Qu X (2011) Colorimetric biosensing using smart materials. Adv Mater 23:4215–4236
26. Lepoitevin M, Lemouel M, Bechelany M, Janot JM, Balme S (2015) Gold nanoparticles for the bare-eye based and spectrophotometric detection of proteins, polynucleotides and DNA. Microchim Acta 182:1223–1229
27. Chen YM, Yu CJ, Cheng TL, Tseng WL (2008) Colorimetric detection of lysozyme based on electrostatic interaction with human serum albumin-modified gold nanoparticles. Langmuir 24:3654–3660
28. Wang W, Wu WY, Zhong XQ, Wang W, Miao Q, Zhu JJ (2011) Aptamer-based PDMS-gold nanoparticle composite as a platform for visual detection of biomolecules with silver enhancement. Biosens Bioelectron 26:3110–3114
29. Su J, Zhou WJ, Xiang Y, Yuan R, Chai YC (2013) Target-induced charge reduction of aptamers for visual detection of lysozyme based on positively charged gold nanoparticles. Chem Commun 49: 7659–7661
30. Frens G (1973) Controlled nucleation for the regulation of the particle size in monodisperse gold suspensions. Nature Phys Sci 241: 20–22
31. Haiss W, Thanh NTK, Aveyard J, Fernig DG (2007) Determination of size and concentration of gold nanoparticles from UV-vis spectra. Anal Chem 79:4215–4221
32. Chen J, Lin Y, Jia L (2015) Preparation of anionic polyelectrolyte modified magnetic nanoparticles for rapid and efficient separation of lysozyme from egg white. J Chromatogr A 1388:43–51
33. Xia F, Zuo X, Yang R, Xiao Y, Kang D, Vallée-Bélisle A, Gong X, Yuen JD, Hsu BBY, Heeger AJ, Plaxco KW (2010) Colorimetric detection of DNA, small molecules, proteins, and ions using unmodified gold nanoparticles and conjugated polyelectrolytes. Proc Natl Acad Sci 107:10837–10841
34. Zheng H, Qiu S, Xu K, Luo L, Song Y, Lin Z, Guo L, Qiu B, Chen G (2013) Colorimetric and fluorometric dual-readout sensor for lysozyme. Analyst 138:6517–6522